Experimental investigation of an integrated renovation solution combining diffuse ceiling ventilation and double skin façade

Zhang, Chen; Larsen, Olena Kalyanova; Hu, Yue; Mikkelsen, Asbjørn Kaagaard; Pedersen, Lotte Louise; Nyborg, Victor Ørsøe; Larsen, Tine Steen

Published in:
Building and Environment

DOI (link to publication from Publisher):
10.1016/j.buildenv.2023.111000

Publication date:
2023

Document Version
Publisher's PDF, also known as Version of record

Building and Environment 246 (2023) 111000

Contents lists available at ScienceDirect

Building and Environment

journal homepage: www.elsevier.com/locate/buildenv

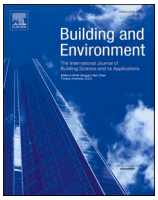

Experimental investigation of an integrated renovation solution combining diffuse ceiling ventilation and double skin façade

Chen Zhang, Olena Kalyanova Larsen *, Yue Hu, Asbjørn Kaagaard Mikkelsen, Lotte Louise Pedersen, Victor Ørsøe Nyborg, Tine Steen Larsen

Department of the Built Environment, Aalborg University, Aalborg, 9220, Denmark

A B S T R A C T

A novel renovation solution was proposed recently by integrating diffuse ceiling ventilation and double skin façade. This study presents an experimental investigation on the performance of the novel solution in a small-scale classroom. The aim of this study was to evaluate the potential in combining the diffuse ceiling ventilation principle with the double-skin façade through the thermal comfort and passive energy performance evaluation in two operation modes: heating mode and cooling mode. The performance of the novel solution was compared to a traditional renovation solution installed in an identical room. The results showed that the novel solution achieved comparable or even superior thermal comfort than traditional renovation solution. In winter, the DSF is able to recover the transmission loss through the glazing and capture the heat gain by solar radiation. The heat recovery rate can reach up to 1.2 when solar radiation was strong. In summer, the air ventilated the DSF cavity and served as an air curtain to remove part of the heat gain. Consequently, it reduces the heat gain to the room and maintains lower indoor temperature than the traditional solution. Benefit of the further activation of thermal mass, the novel solution can reduce the peak operative temperature and shift the peak hour to later of the days. Further research is needed to optimize the system's control strategies and integrate solar shading device in the control strategy.

1. Introduction

In Denmark, only a few schools are newly built, 80 % of the public schools were built before 1980 and most of them with the Energy Label lower than 'D' [1]. About 50 % of the school buildings are ventilated naturally or only with mechanical exhaust [2]. Compared to the other building types, school buildings have significantly higher occupancy density and ventilation demand. There is a high risk of a poor indoor environment associated with the lack of ventilation system or insufficient ventilation rate. A recent study showed that CO_2 concentrations exceed the maximum permissible 1000 ppm in 60 % of the classrooms [1]. Low ventilation rate triggers a significant increase in student absenteeism and has a negative impact on the learning outcome [3–5], as well as children's health and well-being [6–8]. The traditional natural ventilation strategy, for example open windows, easily causes draught in winter or transitional seasons. In order to avoid discomfort, occupants often choose to close the window or reduce the ventilation rate.

To address the issues above, there is a strong need for school renovation to improve the indoor environment and energy performance. Several case studies have been reported in the literatures. Morck et al. [9] described a demonstration school within the EU project 'School of the Future' where the energy renovation measures included installing a new external façade layer, changing the glazing or windows, replacing fluorescent lighting with LEDs, and adding an on-site PV system. Another renovation project of 4 daycare centers reported by Jradi et al. [10], where the renovation solutions included installing demand controlled ventilation, wall and roof insulation, triple glazing windows, and LED light with daylight sensors. The two case studies align with the statistical study by Clausen et al. [11]. By interviewing 366 schools, the four most common renovation areas within the last 10 years are façade/roof (21 %), ventilation (18 %), window (18 %) and lighting (14 %). However, the case studies above indicated that the current renovation solutions require significant intervention in terms of existing construction, and necessary installation space. The construction and installation work can strongly disturb the daily activity and may require occupants to be relocated or renovation to occur during the holiday period. At the same time, to avoid discomfort in the occupied zone, the outdoor air is normally heated via a heat recovery unit and heating coil. It might lead to overheating problem in the classroom even in winter season, due to the high internal load of occupants and equipment [12,13].

A novel renovation concept was proposed in our recent studies [14–16], which has the potential to overcome the limitations of the conventional renovation solutions. It is an integrated solution, which combines double skin façade (DSF) with diffuse ceiling ventilation (DCV). DCV uses a ceiling plenum to distribute air and the fresh air is supplied into the occupied zone through suspended ceiling panels.

* Corresponding author.
E-mail address: ok@build.aau.dk (O.K. Larsen).

https://doi.org/10.1016/j.buildenv.2023.111000
Received 6 June 2023; Received in revised form 27 October 2023; Accepted 30 October 2023
Available online 31 October 2023

Compared to conventional mixing or displacement ventilation systems, DCV can significantly reduce draught risk due to the low momentum air supply [17,18]. In addition, DCV does not require intensive duct work and is able to use low pressure-drop acoustic panel as air diffusers. These features make it easy to implement in the renovation project with low investment cost [19,20], as well as low energy consumption due to the possibility of utilizing natural ventilation and night cooling [21]. However, because DCV directly supply outdoor air into the room, it might lead to high heating demand in winter or even transitional seasons when the outdoor temperature is low or internal heat loads are minimal. DSF concept is known for its potential in preheating the supply air, efficient noise reduction from the outside [22]. Also, from the architectural perspective, DSF appears interesting as an alternative to traditional transparent façade solutions, and at the same time offer high multifunctionality [23]. In this regard DSFs can also be adapted to meet evolving building requirements and changing climatic conditions [24,25]. This adaptability ensures that the renovated building can remain relevant and efficient over time, mitigating the need for further major renovations in the future. Furthermore, DSFs are well-compliant with the passive and active strategies, including Building-Integrated Photovoltaic systems and other novel building-responsive technologies [23]. In terms of building retrofit, DSF solutions can be successfully adopted as a strategy for improved building energy efficiency [23,26,27], even have the potential to resolve structural challenges alongside their primary functions [28].

While DSF systems hold significant appeal, it is important to acknowledge that the methods and tools for evaluating their thermal performance and fluid behavior are not yet fully established [29,30], which may increase the risk of poor performance [31]. Additionally, the high initial investment and maintenance costs have led to a cautious approach among developers when considering the adoption of this technology [24].

The efficiency of building ventilation through a DSF, as a stand-alone solution, can be uncertain in terms of draught risk in the heating season and overheating during summer [32,33]. Therefore, a combination of DSF with DCV, along with efficient design and control of the interface between the plenum and the façade, can enhance named above potentials of DSF application and reduce the risks of poor performance for both systems. The performance of the proposed integrated solution was evaluated in a Danish classroom setting by numerical simulations [14]. Various configurations of the novel solution, encompassing different glazing properties and DSF cavity thicknesses were compared against a range of traditional renovation solutions. The results showed the glazing properties has a significant impact of the system performance than the cavity thickness. The study also demonstrated that the proposed solution can maximize the utilization of the passive cooling and heating resource and save up to 11 % total primary energy consumption compared with the traditional renovation while achieving an equal or even better indoor environmental quality. The performance of the novel solution was further investigated under different boundary conditions [16]. Factors including building orientation, facade properties, future climate change, extreme weather scenarios, and variations in occupant densities were systematically studied. The results revealed that the proposed solution with superior energy performance for southern orientations. It was found that external facade characterized by high thermal mass and low reflectance yields optimal performance. In terms of future climate scenarios, particularly those characterized by mild winters and moderate to hot summers, the novel solution demonstrated superior performance compared to traditional renovation. An equal performance was seen for a varying occupant density.

Although the numerical simulations of the novel solution display promising results, it is crucial to complement these findings through experimental assessments. This study aims to build upon insights gained from simulation-based concept development, as discussed in our previous studies [14,16], by addressing experimentally the areas not fully explored in the simulations. While evaluating the overall energy performance of the integrated solution remains important, it falls beyond the scope of this study. Our primary objective is to conduct an initial concept assessment through evaluation of thermal comfort implications and to review the attainable energy benefits resulting from utilization of passive strategies like pre-heating and self-cooling effects.

The experiments are conducted within a mock-up classroom under nearly realistic operating conditions, enabling a direct comparison between the integrated solution (DSF and DCV) and the traditional classroom renovation approach.

2. Novel solution concept

The principle of the novel solution is to combine two technologies, double skin façade (DSF) and diffuse ceiling ventilation (DCV). To ensure acceptable indoor air quality, a mechanical exhaust is applied in conjunction with DSF and DCV, to supply sufficient ventilation rate through the system. The integrated system could operate in various modes, depending on indoor and outdoor conditions. In this study, two operation modes are tested, namely, heating mode and cooling mode, as illustrated in Fig. 1.

- Heating mode: In this mode, outdoor air enters the DSF cavity from the DSF inlet (1) at the bottom and gradually warms up as it collects solar radiation and heat loss from indoor. The preheated fresh air then enters the DCV plenum (4) and is distributed into the occupied zone through diffuse ceiling panels. An exhaust fan is used to maintain sufficient airflow rate in the room. The airflow through DSF cavity and DCV plenum is driven by mechanical force.
- Cooling mode: In this mode, the outdoor air enters the DSF cavity from the DSF inlet (1). The airflow through the DSF cavity removes the solar heat accumulated in the cavity, and then the heated air can be expelled to the outside through the DSF outlet (2). The airflow through DSF cavity is naturally driven by wind pressure and thermal buoyancy. Meanwhile, the outdoor fresh air is directly supplied through the by-pass opening at the top to the DCV plenum (3 and 4), and further distributed into the occupied zone through diffuse ceiling panels. The airflow through by-pass opening and DCV plenum is driven by mechanical force.

For further information regarding the system's concept and operation modes, please refer to our previous study [14]. It should be noted that detailed control strategies are not implemented in this study, and the focus is on initial testing the potential of seasonal system performance rather than performance optimization.

3. Experiment description

3.1. Test facility

The measurements are conducted in the Two Room Indoor Environment & Energy Universal Facade (TRIUMF) laboratory. The laboratory faces south and is placed on top of the building with no surrounding obstructions, Fig. 2.

The TRIUMF laboratory is separated into two rooms: one room with a traditional renovation solution (reference room) and the other is with the novel renovation solution DSF-DCV (test room). Both rooms have identical floor and roof constructions and are subjected to the same boundary conditions, including the north-facing internal walls (Fig. 3). The test room's position in the floor plan appears different from that of the reference room. Specifically, the reference room is shifted to the south. This adjustment is made to ensure equal solar exposure in both cases. Both rooms share the same interior dimensions of 2.905 m × 2.735 m x 2.735 m, as shown in Fig. 3 (a). The primary distinction between the rooms lies in the presence of an external wall in the reference room: the east-facing wall is exposed to the outdoors. To mitigate the impact of these differences, the east-facing external wall of the reference

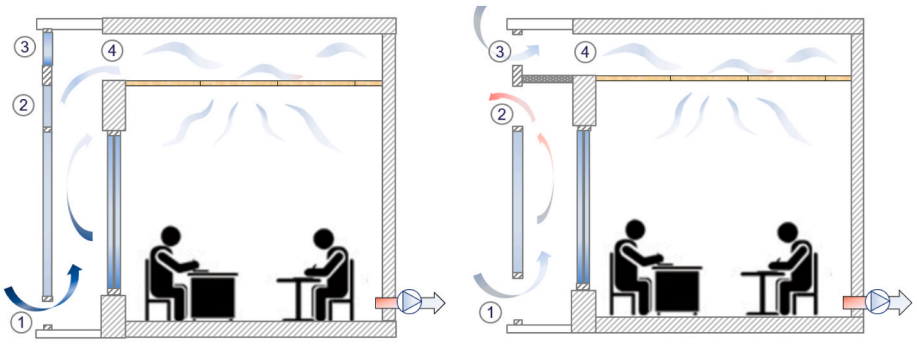

Fig. 1. Concept drawing of DSF-DCV solution with different operation modes ①DSF inlet ②DSF outlet ③By-pass opening ④ DCV plenum inlet (a) Heating mode (b) Cooling mode.

Fig. 2. External facade of the TRIUMF laboratory.

room has been carefully insulated, resulting in U-value of 0.09 W/m^{2}K.

Initially, both rooms had an identical construction of the South-oriented façade element with U-value of 0.30 W/m^{2}K and U-value of the window 1.6 W/m^{2}K. In this study both rooms undergo a transformation, which corresponds to:

- Traditional renovation solution (reference room) which involves replacing windows (resulting U-value 1.32 W/m^{2}K), improving the U-value of the external wall towards South (resulting U-value is 0.18 W/m^{2}K, to meet the Danish building regulation BR18 [34]), and installing balanced mechanical ventilation.
- Novel renovation solution (test room), where the initial façade element with the U-value of 0.30 W/m^{2}K remains unaltered. To that 108 mm of brick is added on the exterior side, to increase the amount of thermal mass in the DSF. Finally, an additional window skin is added to the southern façade forming a ventilated double-skin façade, connected to the diffuse ceiling in the room.

3.2. External façade

Fig. 3 (b) shows the external facade of the measurement facility. DSF external façade consists of 12 windows. 9 small windows are openable which are used to adjust operation modes, and 3 large windows are fixed. The DSF interior façade window has the exact dimensions as the window in the reference room.

Table 1 outlines the window properties.

3.3. Ventilation systems

DCV is installed in the test room, as shown in Fig. 4 (a). It is composed of suspended ceiling panels with 600 mm width, 1200 mm length and 35 mm thickness occupying the entire ceiling area. The ceiling panels are made of wood and cement and are known as cement-bonded wood wool panels, which have good sound-absorbing properties and are penetrable to air. The properties of the diffuse ceiling panels are listed in Table 2. The ventilation system in the test room is not equipped with heating and cooling coils or heat recovery unit. The ventilation supply temperature to the DCV plenum depends on the air temperature through by-pass opening or DSF cavity.

Mixing ventilation is installed in the reference room as a traditional mechanical ventilation solution used in renovation. The inlet is a ceiling mounted diffuser, as shown in Fig. 4 (b). In both rooms, the exhausts are located on the back wall facing the façade, with a diameter of 130 mm. Exhaust fans are utilized in both ventilation systems to keep a constant airflow rate of 6 h^{-1} in the rooms. The ventilation supply temperature is set up to 18 °C in summer, representing the mechanical ventilation with a cooling coil, and 20 °C in winter, representing the mechanical ventilation with heat recovery unit and heating coil.

3.4. Measuring instruments and placements

To evaluate the indoor environment, we measured air temperature, surface temperature, air velocity and airflow rate in both rooms. The measurement equipment and their uncertainty are summary in Table 3. The weather data is obtained from the weather station located on-site.

To measure the air temperature distribution in both rooms, the thermocouples are placed at different heights with several measurement poles, as shown in Fig. 5. The poles are located along the central lines of the rooms with different distances to the façade. To mitigate the influence of solar radiation on the air temperature measurement, the thermocouples exposed to the direct solar radiation are shielded by silver foil.

The air temperatures in the DSF cavity are measured by thermocouples placed in each DSF section to investigate the DSF pre-heating and self-cooling effect, see Fig. 6 (a). Thermocouples in DSF cavity are protected from the influence of direct solar radiation by silver coated and ventilated tube [35], as shown in Fig. 6 (c), air flow through the tube is ensured by a mini fan. In addition, the air temperature from DSF entering DCV plenum are measured by three thermocouples corresponding to each DSF section. The air temperatures in the DCV plenum are also measured to evaluate the temperature distribution and thermal process in the plenum, see Fig. 6 (b).

Surface temperature of walls, floors, diffuse ceiling panels and glazing are measured in both rooms using thermocouples glued to surfaces with a paste of high heat transmission property. To mitigate the influence of direct solar radiation, thermocouples at the glazing surface and wall surface are shielded by silver foil. Air velocities in the rooms are measured by anemometers. The anemometers are placed at different height, and measurement poles are located at various locations within the room to capture both vertical and horizontal velocity profiles, see Fig. 5.

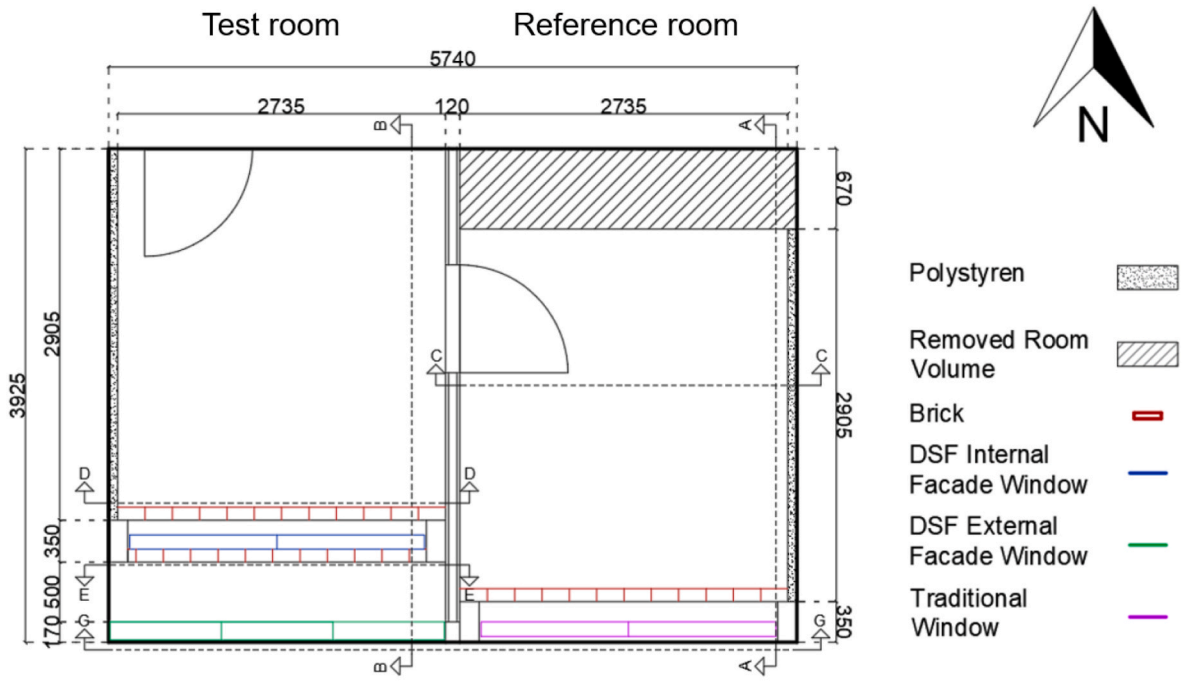

(a)

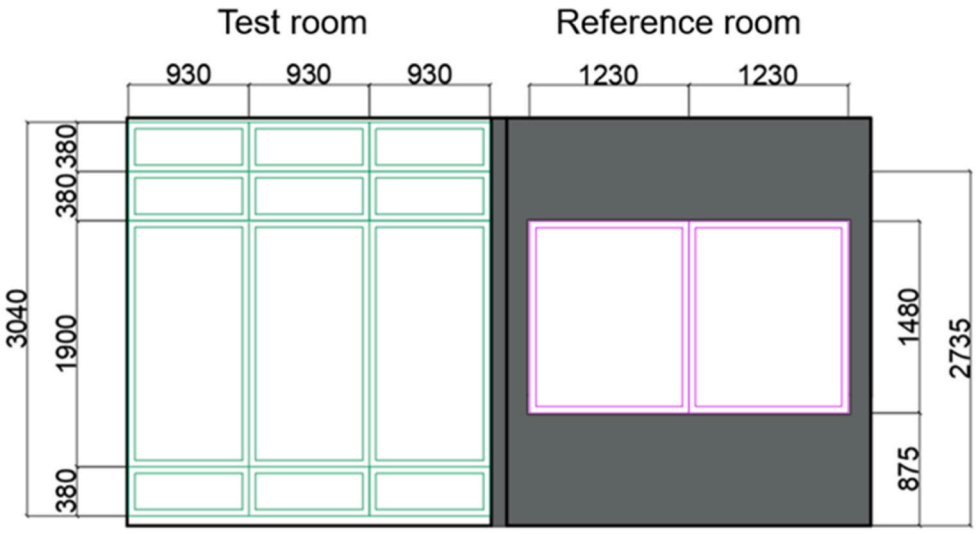

(b)

Fig. 3. Illustration of the measurement facility (a) Plan view (b) External façade. All dimensions in mm.

3.5. Test cases

The case study aims to represent a typical classroom. To simulate internal heat gains from equipment, people, and lighting, four heat sources (black columns with light bulbs inside) are placed symmetrically in each room as shown in Fig. 4. The heat load in both rooms is scaled down based on the room volume to that of a standard classroom, following the guidance for indoor climate in schools [17]. The Danish building regulation [34] recommends that the CO_2 concentration is kept below 1000 ppm for classrooms to achieve a satisfactory atmospheric comfort. The ventilation rate is calculated to fulfill this requirement. The occupied hour in the classroom is 8:00–16:00 to represent a typical school schedule. Two different operation modes are tested under different seasons, as described in Section 2. The summary of test cases and their conditions are described in Table 4.

4. Results

4.1. Heating mode

4.1.1. Thermal comfort

The heating mode was measured for a duration of one week in

Table 1
Window properties. Uw = U-value window, F_f = Frame fraction, g = Solar Heat Gain Coefficient, LT = Light Transmittance.

Window type	Quantity	Area	U_w	F_f	g	LT
	[−]	[m^2]	[W/m^2K]	[−]	[−]	[−]
DSF external small window	9	3.15	1.53	0.63	0.73	0.84
DSF external large window	3	5.31	1.33	0.83	0.73	0.84
DSF internal window	2	3.64	1.6	0.88	0.63	0.8
Traditional renovation window	2	3.64	1.32	0.84	0.73	0.84

Fig. 4. Interior façade and room layout (a) Test room (b) Reference room.

winter, from 7.12.2022 to 14.12.2022. The outdoor temperature ranged from −7.4 °C to 1.3 °C and maximum solar radiation was 311 W/m^2 measured by local weather station, as shown in Fig. 7. No space heating was provided in both rooms to investigate the passive heating effect of the test system. However, the mixing ventilation supply temperature was setup to 20 °C in the reference room, which represented the traditional mechanical ventilation with heat recovery unit and heating coil.

As shown in Fig. 7, the average operative temperature in the test room was around 15 °C, while in the reference room it was about 17 °C. Neither room fulfilled the comfort criteria as recommended by ISO 7730 [36], due to the lack of space heating. However, overheating was observed in both rooms in the noons when the solar radiation was strong, which indicates that shading devices are needed even during winter season to avoid overheating problem. Even though solar radiation plays important roles in both rooms, the mechanisms of heat gain from solar radiation are different. In the reference room, the solar heat gain is transferred through the façade. While, in the test room, heat gain is partly from the solar radiation transmission though DSF, and partly by warming up the ventilation air in the DSF cavity. Therefore, the supply air is already pre-heated in the test room before entering the DCV plenum, as observed from DCV plenum inlet temperature, see Fig. 7. The DCV plenum inlet temperature was influenced by both outdoor temperature and solar radiation. Without solar radiation, the inlet air to DCV plenum was in general 10 °C warmer than outdoor air. While the temperature difference can reach up to 25 °C with solar radiation.

Upon closer inspection of the operative temperature during two sunny days, 7.12–8.12, it can be observed that the slopes of the operative temperature curves differed slightly between the two rooms.

Table 2
Properties of diffuse ceiling panel.

Parameter	Density	Thermal conductivity	Porosity
Unit	kg/m^3	W/m.K	–
Value	359.13	0.085	65 %

Table 3
Measurement equipment and uncertainties.

Variable	Location	Equipment	Uncertainty
Surface temperature	Walls, ceilings, and floors in both rooms DSF glazing DCV Plenum surfaces	Thermocouples type K shielded by silver foil	±0.09 °C
Air temperature	DSF cavity	Thermocouples type K with shielding tubes	±0.09 °C
Air temperature	DCV plenum Occupied zone in both rooms Inlets and exhausts	Thermocouples type K shielded by silver foil	±0.09 °C
Airflow rate	Exhausts	Lindab Ultralink	±5 %
Air velocity	Occupied zones in both room	Anemometers	±2 % for 0–1 m/s ± 5 % for 1–5 m/s

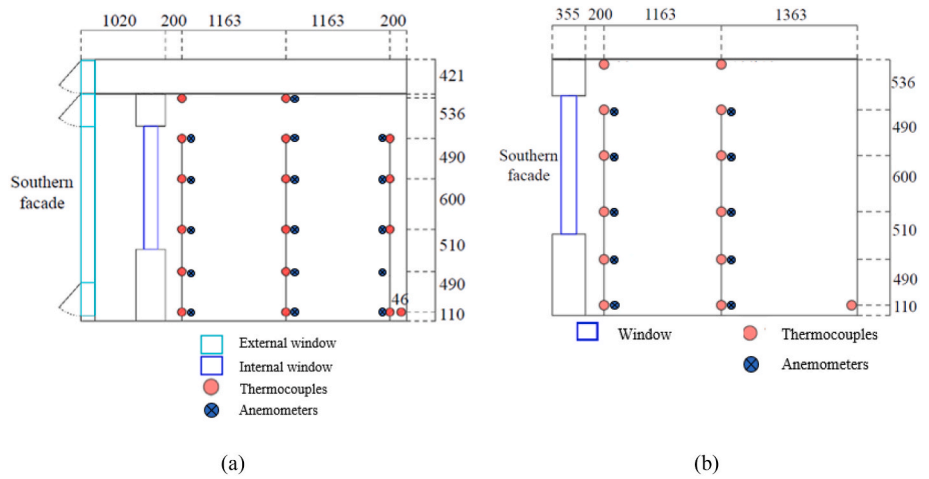

Fig. 5. Air temperature and velocity measurements in both rooms (a) Test room (b) Reference room.

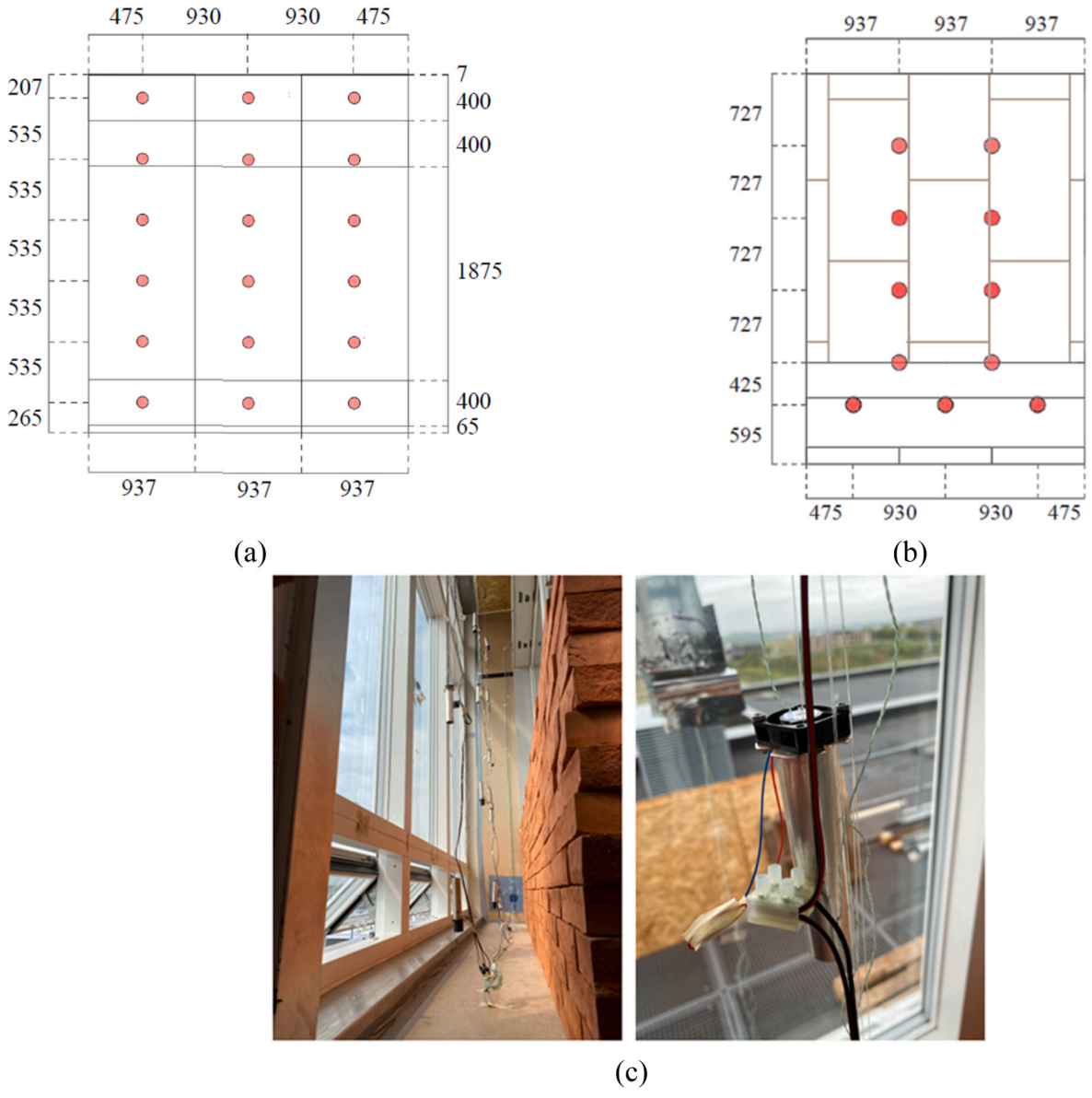

Fig. 6. Air temperature measurement in the integrated solution (a) DSF cavity (b) DCV plenum (c) Thermocouples type K with shielding tubes.

Table 4
Test cases and conditions.

Case	Period	Internal heat load	Ventilation rate	Occupied hour
Heating mode	07.12.2022–14.12.2022	396 W or 50 W/m^2	132 m^3/h or 6h^{-1}	8:00–16:00 (10.12.2022–11.12.2022 are weekend)
Cooling mode	16.06.2022–27.06.2022	396 W or 50 W/m^2	132 m^3/h or 6h^{-1}	8:00–16:00 (20.06-2022-27.06.2022 are holiday)

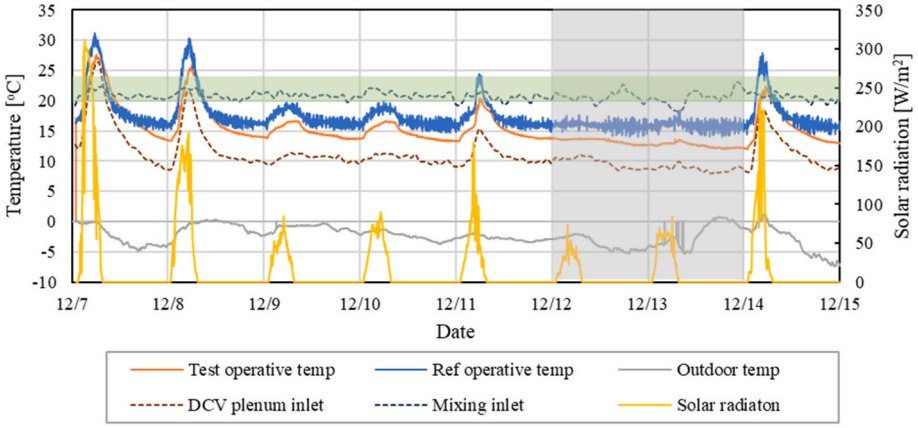

Fig. 7. Operative temperatures and inlet temperatures in both rooms in winter (grey column indicates weekend or holidays; green column indicate comfort criteria recommended by ISO 7730 category B). Solar radiation is the global solar radiation. (For interpretation of the references to colour in this figure legend, the reader is referred to the Web version of this article.)

Specifically, the test room exhibited lower slopes in the operative temperature variation, and the peak temperature hour was shifted when compared with the reference room. This can be attributed to the fact that the ventilated air was compelled to undergo convective heat transfer with ceiling slabs within the DCV plenum, which further activated the thermal mass. The room was cooled down during unoccupied hours due to the low outdoor temperature and lack of heat gains from internal load and solar radiation, which resulted too low operative temperature in the next morning. Ventilation should be turned off during the unoccupied hour to avoid discomfort and save energy in winter season.

The vertical temperature differences between head and ankle were measured in both rooms. Due to the instrument error, the temperature difference in the wall pole was not reported here. As shown in Fig. 8, the vertical temperature differences in both rooms were within the comfort range of 3 °C as recommend by ISO 7730 [36]. A high temperature difference up to 3 °C was observed in the test room on 7th Dec, which was caused by high inlet temperature from W/m2K inlet temperature reached to 26 °C due to the strong solar radiation and low positioned sun. As reported by our previous studies [37,38], a high risk of temperature stratification may occur when DCV supply warm air into the room. Due to the low momentum supply, the warm air will stagnantly stay in the upper zone without entering the occupied zone, which will cause high vertical temperature difference and low air quality in the occupied zone. A good mixing was observed in the test room in the rest of the week, and the vertical temperature difference was less than 0.5 °C. In the reference room, slightly higher vertical temperature differences were observed at the window pole compared to those at the middle pole. This could be due to the downward draught from the cold window surface, resulting in lower air temperatures at ankle level. However, no discomfort was caused by the vertical temperature differences in either room.

The air velocities in the occupied zone in winter were presented in Fig. 9. Based on ISO 7730 [36], the maximum mean air velocity should be lower than 0.16 m/s in winter. In the test room, the max mean velocities were below 0.16 m/s in all the positions except at 0.1 m near the end wall. The velocities in the reference room were similar at all locations, and all of them were within the comfort criteria. No downward draught from the external windows were observed in both rooms.

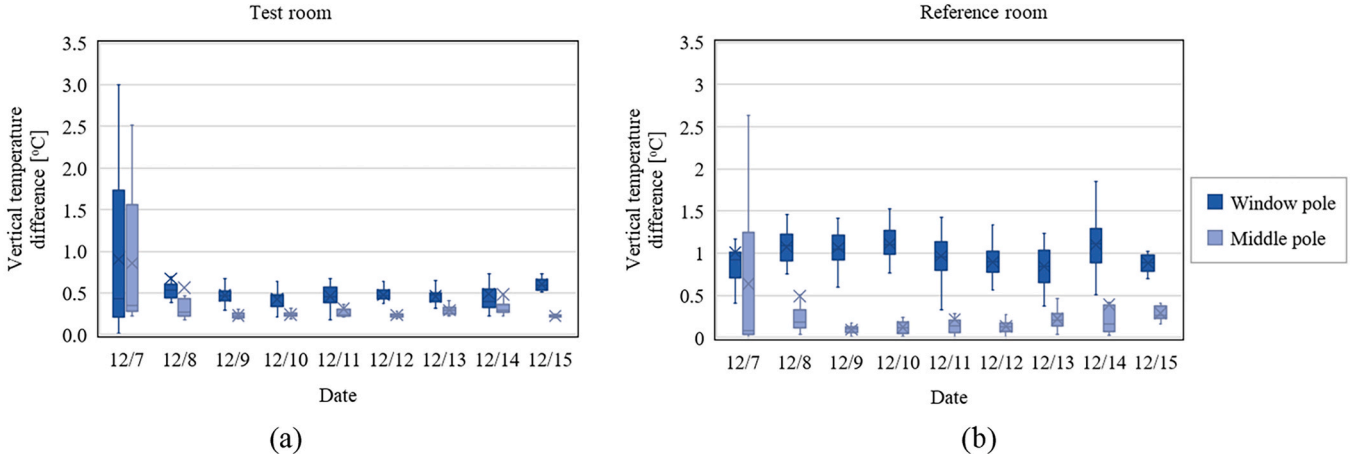

Fig. 8. Vertical temperature difference between head and ankle in winter (grey column indicates weekend or holidays) (a) Test room (b) Reference room.

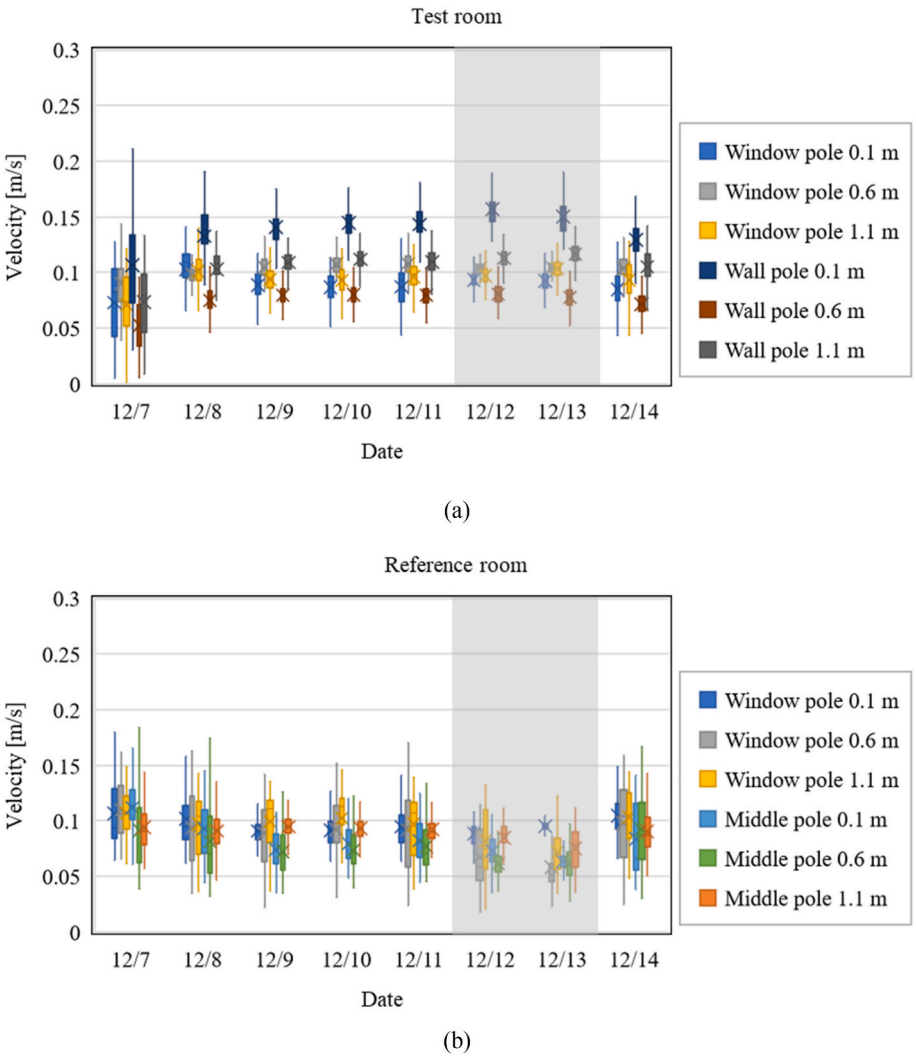

Fig. 9. Air velocity in winter (grey column indicates weekend or holidays) (a) Test room (b) Reference room.

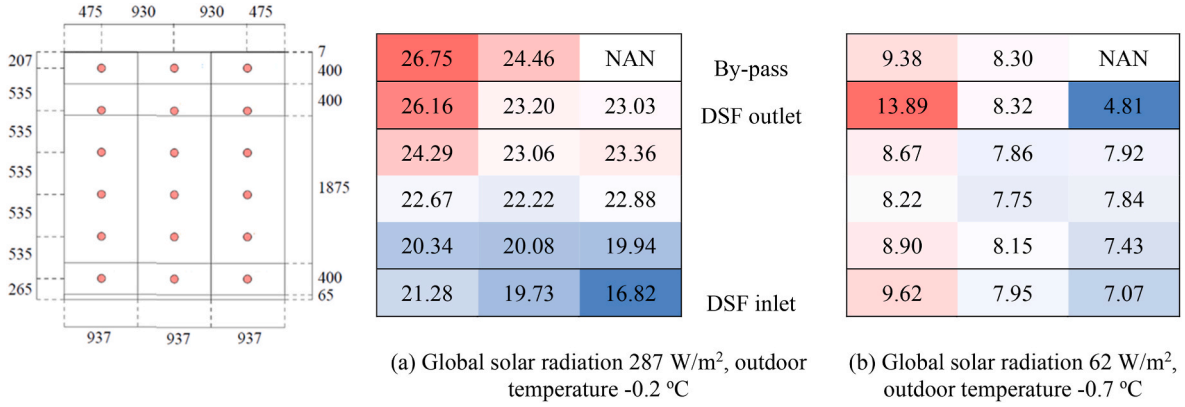

(a) Global solar radiation 287 W/m^2, outdoor temperature -0.2 ºC

(b) Global solar radiation 62 W/m^2, outdoor temperature -0.7 ºC

Fig. 10. Air temperature distribution in the DSF cavity under heating mode (a) Case with high solar radiation (b) Case with low solar radiation (The temperatures are hourly average value at specific hours).

4.1.2. Pre-heating effect of DSF

The pre-heating performance of the tested solution can be observed through the air temperature distribution in the DSF cavity. Two scenarios are analyzed here, one is with high solar radiation, Fig. 10 (a), and the other is with low solar radiation, Fig. 10 (b). During the heating mode operation, outdoor air entered the DSF cavity from the bottom inlet. Although the outdoor temperatures were similar, the air temperatures at the DSF inlet were significantly different in the two scenarios. The DSF inlet was placed in close proximity to a black- W/m2K surrounding of the test and reference room was also painted black, thus resulting in an increase in the local outdoor temperature during sunny conditions.

When the solar radiation was strong, Fig. 10 (a), the outdoor air was warmed up by the surface due to convection before entering the DSF inlet. Therefore, even though the outdoor temperature at the weather station was −0.2 °C, the air temperature was approximate 21 °C at the DSF inlet, and then raised to 26 °C at the top of the cavity. The by-pass opening was closed during the heating mode, the air at the top of DSF cavity entered the DCV plenum and further supplied into the room.

When the solar radiation was low, Fig. 10 (b), the air temperature at DSF inlet was still higher than outdoor temperature but not as much as in the strong radiation scenario. The air was slightly warmed up in the cavity (average 1 °C) mainly by the heat loss from the room. On the other hand, horizontal temperature gradients were observed in both scenarios, which was due to the solar incidence angle and presence of the thermal mass of bricks in the cavity. The solar radiation was from east in the morning and hit the left corner of DSF and caused high air temperature locally.

The pre-heating performance of the DSF could be evaluated by the heat recovery rate, which is calculated by equation (1):

$$HR = \frac{T_{inlet} - T_{outdoor}}{T_{indoor} - T_{outdoor}} \quad (1)$$

Where: HR is heat recovery rate; T_{inlet} is inlet temperature to the DCV plenum; $T_{outdoor}$ is outdoor temperature; T_{indoor} is indoor temperature.

Fig. 11 shows the heat recovery rate of the test solution as a function of global solar radiation during periods of solar exposure. The heat recovery rate reaches up to 1.2. Under dynamic measurement conditions, it is influenced by various parameters, including indoor and outdoor temperatures, the distribution of direct/diffuse solar radiation, wind direction, the shape of the openings, and other factors of heat transfer within the cavity. There is a relationship between the heat recovery rate and global solar radiation, however, the slope is not very significant. The modest slop is partly due to the thermal inertia of the DSF and partly due to the relatively high airflow rate in relation to the DSF cavity size. Despite these complex relations, the results indicated that the system has good pre-heating performance and can supply air to the plenum of the diffuse ceiling at a moderate temperature, thereby reducing the need for implementation of the heat recovery system.

4.2. Cooling mode

4.2.1. Thermal comfort

The cooling mode was measured for a duration of 10 days in summer season, from 16.6.2022 to 27.6.2022, while 21.6.2022–27.6-2022 were holidays and there was no internal heat load in both rooms. The outdoor temperature varied from 10 °C to 28 °C and the maximum solar radiation was 1195 W/m^2, as shown in Fig. 12. The ventilation supply temperature was setup to 18 °C in the reference room, which represents the mechanical ventilation with cooling coil. No mechanical cooling was used in the test room, and no shading device was installed in both rooms.

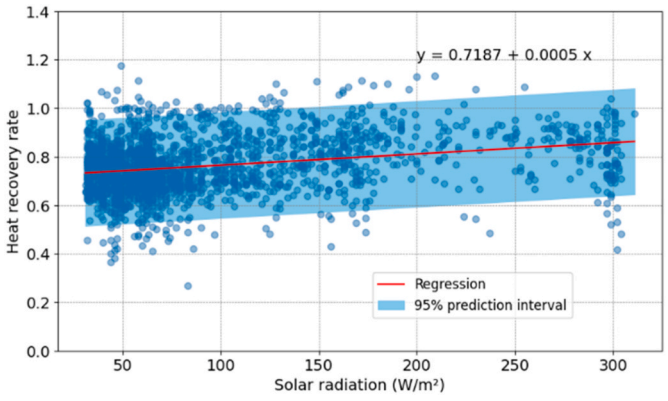

Fig. 11. Heat recovery rate of the test system as a function of global solar radiation for all data points with I_{global}>30 W/m^2.

As shown in Fig. 12, both rooms experienced overheating. Only 19 % of the operating hours in the reference room had the operative temperature within the comfort level category B, while the corresponding value in the test room was 24 %. The impact of solar radiation was more significant in the reference room than the test rooms, with the maximum operative temperature reaching 33 °C in the former and 29.5 °C in the latter. This can be attributed to the fact that ventilation through the DSF cavity removed some of the solar heat gain, but also due to reduced solar heat gain into the room in general, which is caused by the double layer of fenestration in the test room and resulting in the reduced g-value of the combined system. These results underscore the critical role of shading devices in maintaining comfortable indoor temperatures during summer, even with a mechanical cooling system. Similar to the heating mode, the novel system reduced the peak overheating temperature and shifted the peak hour due to the activation of thermal mass.

In the cooling mode, the outdoor air was supplied into the DCV plenum through the by-pass opening located at the top of DSF. Therefore, the inlet temperature to the DCV plenum was directly related with outdoor temperature. There is a high risk of overheating in the test room if the outdoor temperature is above the comfort level, for example 6/25. Even though there was no internal heat load on 6/25, the operative temperature in the test room still reached 28 °C due to the high outdoor temperature and strong solar heat gain.

The vertical temperature differences between head and ankle under cooling mode are shown in Fig. 13. Low vertical temperature difference was observed in both rooms, indicated good mixing was achieved in the occupied zones. In the test room, the vertical temperature difference was less than 0.5 °C and the air temperature was uniform in the horizontal direction as no big variation between the two poles. The vertical temperature difference was slightly higher in the reference room especially near the window, where the maximum values reached 1.9 °C and a larger variation was observed within a day.

The air velocities in the occupied zone in summer season are shown in Fig. 14. In the test room, even though higher air velocities were observed near the window (window pole 0.6 m and 1.1 m), the maximum mean air velocity was 0.16 m/s and still lower than the comfort criteria of 0.19 m/s recommended by ISO 7730 for summer [36]. In the reference room, due to instrument issue, only the air velocities in the middle of the room at height 0.1 m and 0.6 m were recorded. No draught risk was identified in the reference room.

4.2.2. Self-cooling effect of DSF

The self-cooling performance of DSF was investigated in two different summer conditions, see Fig. 15. When the test system operates with cooling mode, the outdoor air enters the cavity from DSF inlet at the bottom and leaves from the DSF outlet in the upper zone. The ventilation is supply through by-pass opening directly into DCV plenum.

Fig. 15 (a) represents the scenario with strong solar radiation, where the solar radiation was 843 W/m^2 and outdoor temperature was 21 °C. The air in the DSF cavity was warmed up by solar radiation to approximate 35 °C, especially in the middle of the cavity. The air ventilated the DSF cavity and severed as an air curtain to remove part of the heat gain out of the cavity, as the mean air temperature decreased to 31 °C at the DSF outlet. However, there was still a large part of solar heat gain transmitted through glazing to the room. Fig. 15 (b) represents the scenario with low solar radiation of 35 W/m^2 and outdoor temperature was 14.5 °C. The air temperature distribution was rather uniform in the DSF cavity, and a slightly higher air temperature was observed at the left side due to the incidence angle of the solar radiation. In both cases, the air temperature at the by-pass opening was strongly determined by the outdoor temperature. However, the solar radiation still had certain impact on the supply air temperature because the air could be warmed up by the black-painted surface before entering the by-pass opening (see Fig. 2). It indicated the thermal mass and absorptance of external façade

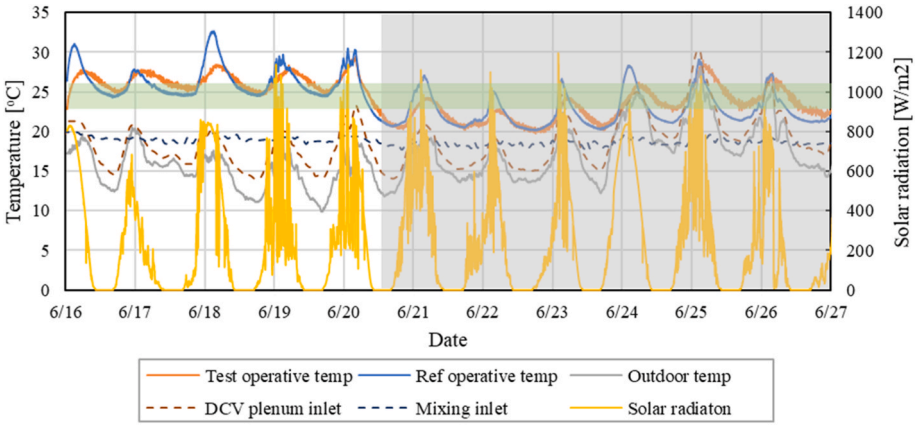

Fig. 12. Operative temperatures and inlet temperatures in both rooms in summer (grey column indicates weekend or holidays; green column indicate comfort criteria recommended by ISO 7730 category B). (For interpretation of the references to colour in this figure legend, the reader is referred to the Web version of this article.)

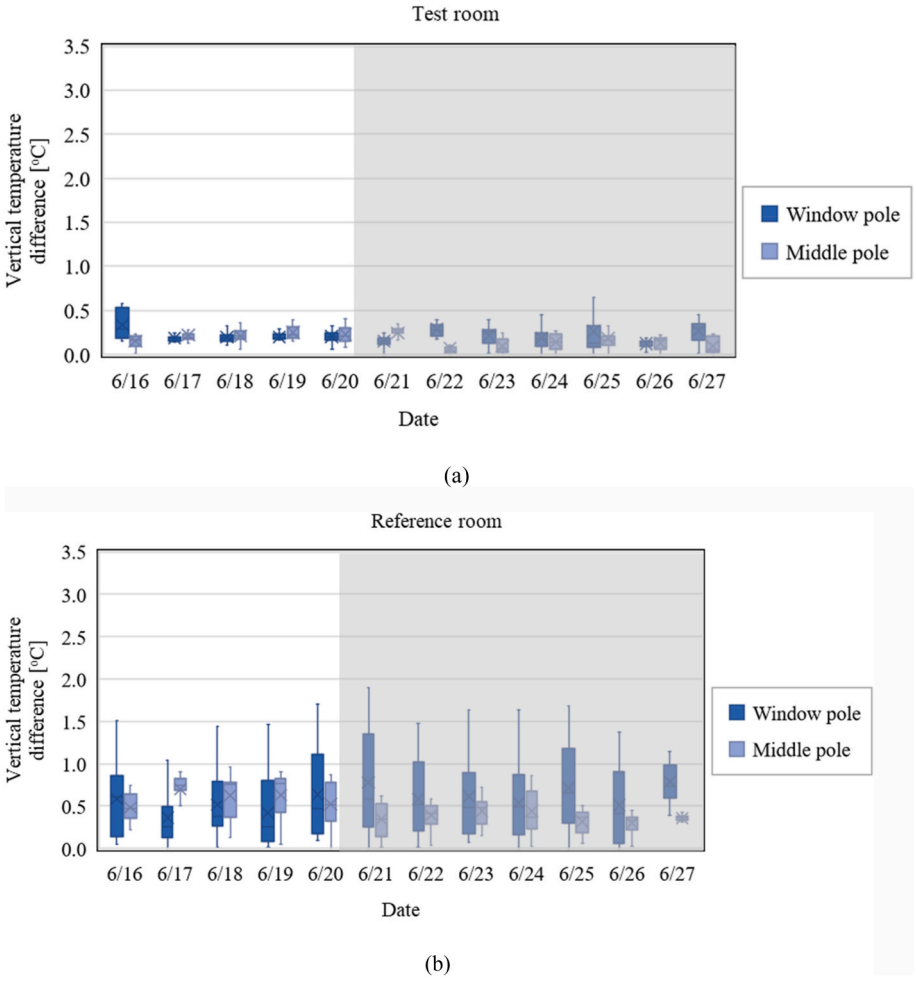

Fig. 13. Vertical temperature difference between head and ankle in summer (a) Test room (b) Reference room.

play an important role to the system performance, which was observed by our previous simulation study [16].

5. Discussion and conclusion

This study presents an experimental investigation on the performance of a novel renovation solution integrating DSF and DCV in a small-scale classroom. The performance was evaluated in term of thermal comfort and passive energy effect under 2 scenarios, with different operation modes and weather conditions. A traditional renovation solution was installed in an identical room and measured during the same period, which was used as reference cases.

The results showed that the novel solution achieved comparable or even superior thermal comfort than traditional renovation solution,

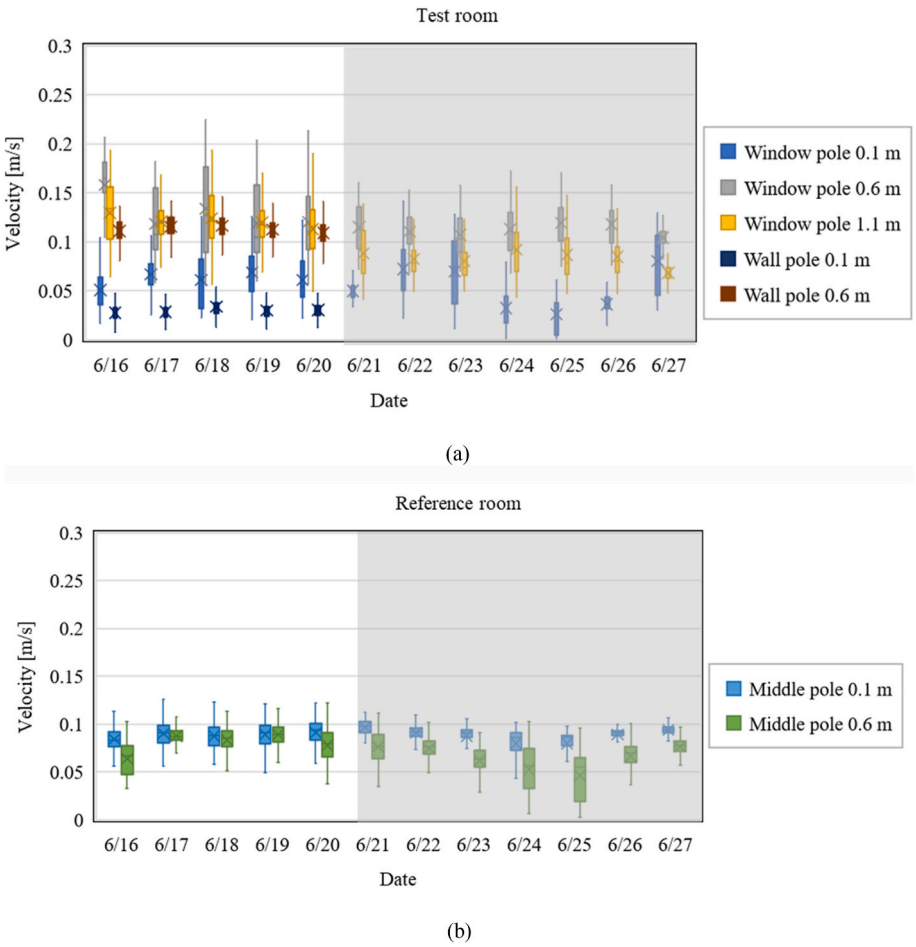

Fig. 14. Air velocity in summer (a) Test room (b) Reference room.

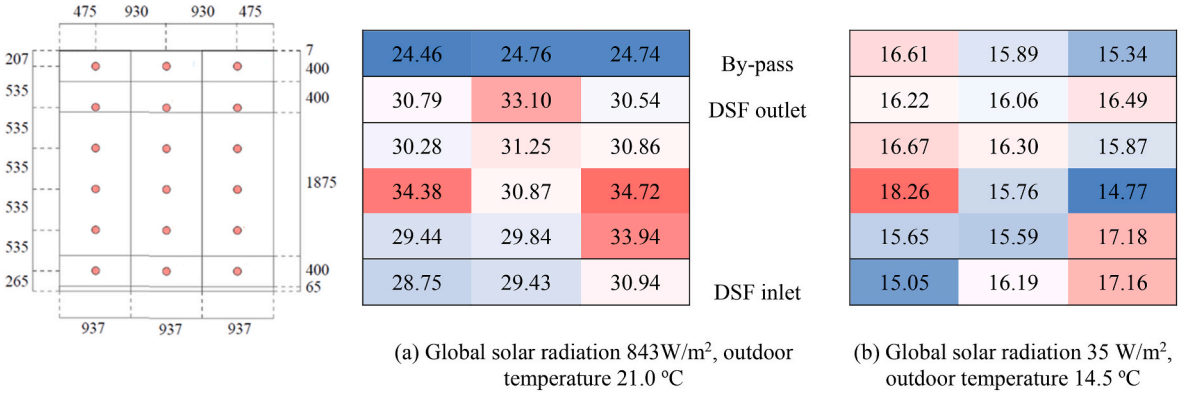

(a) Global solar radiation 843W/m^2, outdoor temperature 21.0 °C

(b) Global solar radiation 35 W/m^2, outdoor temperature 14.5 °C

Fig. 15. Air temperature distribution in the DSF cavity under cooling mode (a) Case with high solar radiation (b) Case with low solar radiation.

while consuming less energy. In winter, neither solution could provide comfort indoor temperature during entire occupied hours due to the absence of space heating. On the other hand, overheating problem was observed in both rooms in winter when solar radiation was strong. Compared with the traditional solution, the novel solution can reduce the peak operative temperature and shift the peak hour to later of the days, because the ventilation was forced to go through DCV plenum and enabled to further activate the thermal mass of ceiling slabs.

In summer, the novel solution provided more comfort hours than the traditional solution. However, both rooms suffered from significant overheating due to the absence of shading devices. The novel solution was able to reduce the peak operative temperature in summer by expelling a portion of the solar gain from the ventilated cavity to outside, and the activation of thermal mass mitigated the peak operative temperature and shift the peak hour similar to the winter scenario.

In terms of local comfort, the test room with novel solution exhibited a low vertical temperature gradient for most of the measurement period. However, there is a risk of temperature stratification when supply warmer air by diffuse ceiling ventilation, due to the low momentum from the inlet. Low draught was observed in all scenarios.

Energy efficiency is a key consideration in building design, the novel solution presented a high potential on utilization of natural and passive

resources. In winter, the DSF is able to recover the transmission loss through the glazing and capture the heat gain by solar radiation, despite the absence of a heat recovery unit. The heat recovery rate can reach up to 1.2 when solar radiation was strong. In summer, the air ventilated the DSF cavity and severed as an air curtain to remove part of the heat gain. Consequently, it can reduce the heat gain to the room and maintain lower indoor temperature than the traditional solution.

The performance of the novel solution is more sensitive to the outdoor and indoor conditions, as well as design parameters compared with the traditional solution, which was also documented by our numerical studies [14,16]. For example, the optical properties (absorbance)of material of external façade play an important role in the system's performance. The outdoor air might be warmed up by the external façade before entering DSF cavity or DCV plenum, which could have opposite impacts in winter and summer season. The simulation results show that the dark surface with (high absorptance) could significantly reduce the heating demand in winter but lead to a high overheating risk in summer. Furthermore, the passive cooling effect can only work when the outdoor temperature is lower than 18 °C. When the outdoor temperature is high, the system can not remove the surplus heat out of the room due to the lack of natural cooling capacity.

At least, the measured results indicate seasonal control is not enough for the novel solution. An advanced control strategy should be developed by considering the real-time variations (hourly or even higher time interval) on weather condition (outdoor temperature, solar radiation) and indoor condition (occupant density and schedule). Solar shading device should be applied and included in the advanced control.

6. Limitations and future study

The current study presented several limitations. First of all, the ventilation effectiveness regarding the air quality was not investigated, since no contaminant sources were setup in this study. Therefore, the ventilation rate was kept constant and same values in both rooms and no measurement on the fan power neither. Secondly, the primary focus of this study was on assessing thermal comfort implications and exploring the attainable energy benefits of passive strategies, such as pre-heating and self-cooling effects, Therefore, the study does not include a comprehensive evaluation of the overall energy performance of the integrated solution when compare against the traditional renovation solution. The broader analysis of the integrated solution's overall energy efficiency is not within the scope of this research. This limitation should be considered when interpreting the findings of this work, as a more comprehensive assessment of energy performance, but also the draught rate may be necessary for a complete understanding of the system's capabilities and limitations. This expanded evaluation should encompass not only air velocity but also air temperature to provide a fair assessment of the draught rate. Finally, this study did not delve into the specifics of control strategies, it contributes to the broader knowledge and understanding of the system's performance under different operation modes and conditions. Further research is needed to optimize the system's control strategies to achieve optimal energy efficiency and indoor environmental quality.

Declaration

During the preparation of this work the authors used GPT-3.5 developed by OpenAI, to assist in proofreading, and to improve language and readability. After using this tool the authors reviewed and edited the content as needed and take responsibility for the content of the publication.

CRediT authorship contribution statement

Chen Zhang: Writing – review & editing, Writing – original draft, Visualization, Validation, Supervision, Resources, Project administration, Methodology, Investigation, Funding acquisition, Formal analysis, Data curation, Conceptualization. **Olena Kalyanova Larsen:** Writing – review & editing, Validation, Supervision, Resources, Project administration, Methodology, Funding acquisition, Conceptualization. **Yue Hu:** Investigation, Data curation. **Asbjørn Kaagaard Mikkelsen:** Investigation, Formal analysis, Data curation. **Lotte Louise Pedersen:** Investigation, Formal analysis, Data curation. **Victor Ørsøe Nyborg:** Investigation, Formal analysis, Data curation. **Tine Steen Larsen:** Writing – review & editing.

Declaration of competing interest

The authors declare the following financial interests/personal relationships which may be considered as potential competing interests: Olena Kalyanova Larsen reports financial support was provided by Energy Technology Development and Demonstration Program (EUDP), Denmark.

Data availability

Data will be made available on request.

Acknowledgement

This work has been supported by the Energy Technology Development and Demonstration Program (EUDP), Denmark under the name I-DIFFER (Journal number: 64020-2140).

References

[1] Realdania, OVERSIGT OVER SKOLERENOVERINGER MED FOKUS PÅ AT SKABE BEDRE INDEKLIMA, 2016 [Online], https://realdania.dk/publikationer/faglige-publikationer/indeklimaiskoler.
[2] J. Toftum, B.U. Kjeldsen, P. Wargocki, H.R. Menå, E.M.N. Hansen, G. Clausen, Association between classroom ventilation mode and learning outcome in Danish schools, Build. Environ. 92 (2015) 494–503, https://doi.org/10.1016/j.buildenv.2015.05.017.
[3] P. Wargocki, J.A. Porras-Salazar, S. Contreras-Espinoza, The relationship between classroom temperature and children's performance in school, Build. Environ. 157 (Jun. 2019) 197–204, https://doi.org/10.1016/J.BUILDENV.2019.04.046.
[4] P. Wargocki, J.A. Porras-Salazar, S. Contreras-Espinoza, W. Bahnfleth, The relationships between classroom air quality and children's performance in school, Build. Environ. 173 (2020), https://doi.org/10.1016/j.buildenv.2020.106749. February.
[5] J. Woo, P. Rajagopalan, M.M. Andamon, An evaluation of measured indoor conditions and student performance using d2 Test of Attention, Build. Environ. 214 (2022), 108940, https://doi.org/10.1016/j.buildenv.2022.108940. November 2021.
[6] T. Salthammer, et al., Children's well-being at schools: impact of climatic conditions and air pollution, Environ. Int. 94 (2016) 196–210, https://doi.org/10.1016/J.ENVINT.2016.05.009. Sep.
[7] A.M. Sadick, M.H. Issa, Occupants' indoor environmental quality satisfaction factors as measures of school teachers' well-being, Build. Environ. 119 (2017) 99–109, https://doi.org/10.1016/j.buildenv.2017.03.045.
[8] M. Szabados, et al., Association of parent-reported health symptoms with indoor air quality in primary school buildings – the InAirQ study, Build. Environ. 221 (2022), https://doi.org/10.1016/j.buildenv.2022.109339. June.
[9] O. Morck, K.E. Thomsen, B.E. Jorgensen, School of the future: deep energy renovation of the hedegaards school in Denmark, Energy Proc. 78 (2015) 3324–3329, https://doi.org/10.1016/j.egypro.2015.11.745.
[10] M. Jradi, C.T. Veje, B.N. Jørgensen, A dynamic energy performance-driven approach for assessment of buildings energy Renovation—Danish case studies, Energy Build. 158 (2018) 62–76, https://doi.org/10.1016/j.enbuild.2017.09.094.
[11] G. Clausen, J. Toftum, G. Bekö, E.P. Dam-Krogh, A.B. Fangel, K. Andersen, Indeklima I Skoler, Realdania, 2017.
[12] C. Zhang, P.K. Heiselberg, M. Pomianowski, T. Yu, R.L. Jensen, Experimental study of diffuse ceiling ventilation coupled with a thermally activated building construction in an office room, Energy Build. 105 (2015) 60–70, https://doi.org/10.1016/j.enbuild.2015.07.048.
[13] T. Yu, P. Heiselberg, B. Lei, M. Pomianowski, C. Zhang, A novel system solution for cooling and ventilation in office buildings: a review of applied technologies and a case study, Energy Build. 90 (2015), https://doi.org/10.1016/j.enbuild.2014.12.057.
[14] L.A. Bugenings, M. Schaffer, O.K. Larsen, C. Zhang, A novel solution for school renovations: combining diffuse ceiling ventilation with double skin facade, J. Build. Eng. 49 (2022), 104026, https://doi.org/10.1016/j.jobe.2022.104026. January.

[15] G.T. Tranholm, et al., Helhedsorienteret Og Skånsom Energi- Og Indeklimarenovering, HVAC magasinet, 2022, pp. 60–62.
[16] M. Schaffer, L.A. Bugenings, O.K. Larsen, C. Zhang, Exploring the potential of combining diffuse ceiling and double-skin facade for school renovations, Build. Environ. 235 (January) (2023), 110199, https://doi.org/10.1016/j.buildenv.2023.110199.
[17] J. Fan, C.A. Hviid, H. Yang, Performance analysis of a new design of office diffuse ceiling ventilation system, Energy Build. 59 (Apr. 2013) 73–81, https://doi.org/10.1016/j.enbuild.2013.01.001.
[18] W. Wu, et al., Diffuse ceiling ventilation for buildings: a review of fundamental theories and research methodologies, J. Clean. Prod. 211 (2018) 1600–1619, https://doi.org/10.1016/J.JCLEPRO.2018.11.148.
[19] C. Zhang, P. Heiselberg, P.V. Nielsen, Diffuse ceiling ventilation - a review, Int. J. Vent. 13 (1) (2014).
[20] C. Zhang, T. Yu, P. Heiselberg, M. Pominaowski, P. Nielsen, Diffuse ceiling ventilation: design guide, DCE Techincal Rep 27 (2016), https://doi.org/10.13140/RG.2.2.25455.43684.
[21] C.A. Hviid, S. Petersen, Integrated Ventilation and Night Cooling in Classrooms with Diffuse Ceiling Ventilation, 11Th Ökosan, 2011.
[22] D. Saelens, J. Carmeliet, H. Hens, Energy performance assessment of multiple-skin facades, HVAC R Res. 9 (2) (2003) 167–185, https://doi.org/10.1080/10789669.2003.10391063.
[23] F. Ascione, N. Bianco, T. Iovane, M. Mastellone, G.M. Mauro, The evolution of building energy retrofit via double-skin and responsive façades: a review, Sol. Energy 224 (2021) 703–717, https://doi.org/10.1016/j.solener.2021.06.035. June.
[24] R.C.G.M. Loonen, M. Trčka, D. Cóstola, J.L.M. Hensen, Climate adaptive building shells: state-of-the-art and future challenges, Renew. Sustain. Energy Rev. 25 (2013) 483–493, https://doi.org/10.1016/j.rser.2013.04.016.
[25] C. Zhang, et al., Resilient cooling strategies – a critical review and qualitative assessment, Energy Build. 251 (2021), 111312, https://doi.org/10.1016/j.enbuild.2021.111312.
[26] A. Fallahi, F. Haghighat, H. Elsadi, Energy performance assessment of double-skin façade with thermal mass, Energy Build. 42 (9) (2010) 1499–1509, https://doi.org/10.1016/j.enbuild.2010.03.020.
[27] M. Wang, et al., Comparison of energy performance between PV double skin facades and PV insulating glass units, Appl. Energy 194 (2017) 148–160, https://doi.org/10.1016/j.apenergy.2017.03.019.
[28] G. Aruta, F. Ascione, N. Bianco, T. Iovane, G.M. Mauro, A responsive double-skin façade for the retrofit of existing buildings: analysis on an office building in a Mediterranean climate, Energy Build. 284 (2023), 112850, https://doi.org/10.1016/j.enbuild.2023.112850.
[29] A. Dama, D. Angeli, O.K. Larsen, Naturally ventilated double-skin façade in modeling and experiments, Energy Build. 144 (2017) 17–29, https://doi.org/10.1016/j.enbuild.2017.03.038.
[30] S. Preet, J. Mathur, S. Mathur, Influence of geometric design parameters of double skin façade on its thermal and fluid dynamics behavior: a comprehensive review, Sol. Energy 236 (2022) 249–279, https://doi.org/10.1016/j.solener.2022.02.055. February.
[31] S.P. Melgaard, I.T. Nikolaisson, C. Zhang, H. Johra, O.K. Larsen, Double-skin façade simulation with computational fluid dynamics : a review of simulation trends , validation methods and research gaps, Build. Simulat. (2023), https://doi.org/10.1007/s12273-023-1052-y.
[32] F. Pomponi, P.A.E. Piroozfar, R. Southall, P. Ashton, E.R.P. Farr, Energy performance of Double-Skin Façades in temperate climates: a systematic review and meta-analysis, Renew. Sustain. Energy Rev. 54 (Feb. 2016) 1525–1536, https://doi.org/10.1016/J.RSER.2015.10.075.
[33] K. Pelletier, C. Wood, J. Calautit, Y. Wu, The viability of double-skin façade systems in the 21st century: a systematic review and meta-analysis of the nexus of factors affecting ventilation and thermal performance, and building integration, Build. Environ. 228 (September 2022) (2023), 109870, https://doi.org/10.1016/j.buildenv.2022.109870.
[34] The Danish Ministry of Economic and Business Affairs, in: BR18: Energikrav Ved Ombygninger Og Udskiftning Af Bygningsdele, 2022. Accessed: Sep. 30, https://bygningsreglementet.dk/Historisk/BR18_Version8.
[35] O. Kalyanova, F. Zanghirella, P. Heiselberg, M. Perino, R.L. Jensen, Measuring air temperature in glazed ventilated facades in the presence of direct solar radiation, in: The International Conference on Air Distribution in Rooms, Roomvent., 2007.
[36] International Standard, ISO 7730:2005 Ergonomics of the Thermal Environment – Analytical Determination and Interpretation of Thermal Comfort Using Calculation of the PMV and PPD Indices and Local Thermal Comfort Criteria, 2005.
[37] C. Zhang, P. Heiselberg, P. V Nielsen, Diffuse ceiling ventilation : a review, Int. J. Vent. 13 (1) (2014) 49–63.
[38] C. Zhang, T. Yu, P. Heiselberg, M. Pominaowski, P. Nielsen, Diffuse Ceiling Ventilation – Design Guide, Aalborg University, DCE Techincal Report, 2016.